Inorg. Chem. **2003**, *42*, 1549–1555

Lanthanum Gallium Bismuthide, $LaGaBi_2$

Mark G. Morgan, Meitian Wang, Wing Yan Chan, and Arthur Mar*

Department of Chemistry, University of Alberta, Edmonton, Alberta, Canada T6G 2G2

Received June 18, 2002

The ternary rare-earth gallium bismuthide $LaGaBi_2$ has been prepared through reaction of the elements. Its structure (Pearson symbol *hP*24, hexagonal, space group *P*6/*mmm*, $Z = 6$, $a = 13.5483(4)$ Å, $c = 4.3937(1)$ Å) contains columns of La_6 trigonal prisms centered by Bi atoms. These columns are surrounded by a framework consisting of three-atom-wide Bi ribbons and Ga_6 rings. Additional Bi atoms are sandwiched between pairs of Ga_6 rings. $LaGaBi_2$ is structurally closely related to $La_{13}Ga_8Sb_{21}$. A retrotheoretical analysis of the structure through extended Hückel band structure calculations suggests an interesting electronic situation in which strong multiple bonding in the Ga–Ga network coexists with weak hypervalent bonding in the Bi–Bi network and confirms the metallic behavior seen in electrical resistivity measurements.

Introduction

There are relatively few known polybismuthides, compounds in which Bi formally assumes a negative oxidation state and engages in homoatomic Bi−Bi bonding. In some situations, the Bi substructure can be explained by normal 2c−2e$^-$ bonds, as in $Ca_5Al_2Bi_6$ containing singly bonded Bi−Bi pairs,[1] and in alkaline-earth bismuthides $A_{11}Bi_{10}$ (A = Ca, Sr, Ba) containing Bi_2^{4-} dumbbells and Bi_4^{4-} squares in addition to isolated Bi^{3-} anions.[2−4] $PtBi_2$ also contains Bi−Bi pairs, but the higher electronegativity of Pt compared to Bi renders a negative oxidation state of Bi doubtful.[5] Multiple bonding has been invoked in some alkali-metal bismuthides such as Cs_3Bi_2 and A_5Bi_4 (A = K, Rb, Cs).[6,7] In other situations, hypervalent Bi−Bi bonding is operative, as in ternary alkaline-earth transition-metal bismuthides $AMBi_2$ (A = Ca, Sr, Ba; M = Mn, Zn, Cd)[8−11] and rare-earth transition-metal bismuthides (RE)M_2Bi_2 (RE = rare earth; M = Ni, Pd) and $CeCu_{1-x}Bi_2$ containing $^2_\infty$[Bi] square sheets,[12−14] in $A_{14}MBi_{11}$ compounds such as $Eu_{14}MnBi_{11}$ containing Bi_3^{7-} linear trimers,[15] and perhaps in Ti_8Bi_9 and Hf_8Bi_9 containing a 3D network of connected Bi squares.[16] $ZrBi_2$ and $HfBi_2$ represent interesting cases in which a six-atom-wide Bi ribbon is found.[17,18]

We have been investigating ternary RE−M−Sb systems (where M is a main-group element from group 13 or 14) in which the occurrence of Sb ribbons excised as fragments of a square net serves as a structural organizing principle.[19] In many circumstances, the bonding in these remarkably complex structures can still be understood in terms of the Zintl concept, notwithstanding the reduced electronegativity differences that would render questionable its application. If the corresponding systems with Bi, which is less electronegative than Sb, are examined, there are very few examples found: $Eu_{14}InBi_{11}$ conforms to the Zintl concept,[15] whereas La_4SnBi_2 and $La_4Pb_xBi_{3-x}$, which are typical intermetallic phases adopting the anti-Th_3P_4-type structure, do

* To whom correspondence should be addressed. Telephone: (780) 492-5592. Fax: (780) 492-8231. E-mail: arthur.mar@ualberta.ca.

(1) Cordier, G.; Schäfer, H.; Stelter, M. *Z. Naturforsch. B: Anorg. Chem. Org. Chem.* **1984**, *39*, 727.
(2) Deller, K.; Eisenmann, B. *Z. Naturforsch. B: Anorg. Chem. Org. Chem.* **1976**, *31*, 29.
(3) Merlo, F.; Fornasini, M. L. *Mater. Res. Bull.* **1994**, *29*, 149.
(4) Derrien, G.; Tillard-Charbonnel, M.; Manteghetti, A.; Monconduit, L.; Belin, C. *J. Solid State Chem.* **2002**, *164*, 169.
(5) Brese, N. E.; von Schnering, H. G. *Z. Anorg. Allg. Chem.* **1994**, *620*, 393.
(6) Gascoin, F.; Sevov, S. C. *J. Am. Chem. Soc.* **2000**, *122*, 10251.
(7) Gascoin, F.; Sevov, S. C. *Inorg. Chem.* **2001**, *40*, 5177.
(8) Cordier, G.; Eisenmann, B.; Schäfer, H. *Z. Anorg. Allg. Chem.* **1976**, *426*, 205.
(9) Cordier, G.; Schäfer, H. *Z. Naturforsch. B: Anorg. Chem. Org. Chem.* **1977**, *32*, 383.
(10) Brechtel, E.; Cordier, G.; Schäfer, H. *Z. Naturforsch. B: Anorg. Chem. Org. Chem.* **1980**, *35*, 1.
(11) Brechtel, E.; Cordier, G.; Schäfer, H. *J. Less-Common Met.* **1981**, *79*, 131.
(12) Hofmann, W. K.; Jeitschko, W. *J. Less-Common Met.* **1988**, *138*, 313.
(13) Hofmann, W. K.; Jeitschko, W. *Monatsh. Chem.* **1985**, *116*, 569.
(14) Ye, J.; Huang, Y. K.; Kadowaki, K.; Matsumoto, T. *Acta Crystallogr., Sect. C: Cryst. Struct. Commun.* **1996**, *52*, 1323.
(15) Chan, J. Y.; Wang, M. E.; Rehr, A.; Kauzlarich, S. M.; Webb, D. J. *Chem. Mater.* **1997**, *9*, 2131, and references therein.
(16) Richter, C. G.; Jeitschko, W. *J. Solid State Chem.* **1997**, *134*, 26.
(17) Eberle, D.; Schubert, K. *Z. Metallkd.* **1968**, *59*, 306.
(18) Haase, M. G.; Block, H.; Jeitschko, W. *Z. Anorg. Allg. Chem.* **2001**, *627*, 1941.
(19) Mills, A. M.; Lam, R.; Ferguson, M. J.; Deakin, L.; Mar, A. *Coord. Chem. Rev.* **2002**, *233−234*, 207.

10.1021/ic020413w CCC: $25.00
Published on Web 02/13/2003

Table 1. Crystallographic Data for $LaGaBi_2$

fw	626.59	T, °C	22
space group	D_{6h}^1−$P6/mmm$ (No. 191)	λ, Å	0.710 73
a, Å	13.5483(4)	ρ_{calcd}, g cm^{-3}	8.938
c, Å	4.3937(1)	μ(Mo Kα), cm^{-1}	898.57
V, Å^3	698.44(3)	$R(F)$ for $F_o^2 > 2\sigma(F_o^2)^a$	0.037
Z	6	$R_w(F_o^2)^b$	0.076

^{a} $R(F) = \sum||F_o| - |F_c||/\sum|F_o|$. ^{b} $R_w(F_o^2) = [\sum[w(F_o^2 - F_c^2)^2]/\sum wF_o^4]^{1/2}$; $w^{-1} = [\sigma^2(F_o^2) + (0.0412p)^2]$, where $p = [\max(F_o^2,0) + 2F_c^2]/3$.

not.[20] We therefore embarked on the challenge to prepare ternary rare-earth main-group bismuthides RE−M−Bi (M = group 13 or 14) to see if Bi ribbons would also emerge as a structural feature in these compounds. Reported here is the first rare-earth gallium bismuthide, $LaGaBi_2$, containing Bi ribbons that are reminiscent of the Sb ribbons found in the closely related structures of $La_{13}Ga_8Sb_{21}$ and La_6MnSb_{15}.[21,22] The bonding in $LaGaBi_2$ is examined through a retrotheoretical analysis, and a resistivity measurement is presented.

Experimental Section

Synthesis. La powder (99.9%, Cerac), Bi powder (99.999%, Cerac), and crushed Ga granules (99.9999%, Alfa-Aesar) were used as starting materials and handled under an argon atmosphere. Reactions were carried out on a 0.25 g scale in evacuated fused-silica tubes (8 cm length; 10 mm i.d.). The reactants were heated at 950 °C for 3 days, cooled slowly to 500 °C over 2 days, and then cooled to 20 °C over 24 h. Black needle-shaped crystals of $LaGaBi_2$ were obtained with use of the stoichiometric ratio La:Ga:Bi = 1:1:2, but crystallinity and yields were improved when the ratio is 1:2:1, presumably with excess Ga serving as a flux. Windowless EDX (energy-dispersive X-ray) analyses were performed on two separate instruments, a Hitachi S-2700 and a JEOL JSM-6301 FXV scanning electron microscope. These crystals contained 21(2)% La, 27(2)% Ga, and 52(4)% Bi (average of 16 analyses). When a 1:1 mixture of La and Bi powder was used as a calibration standard for the EDX analyses, the crystal selected for the structure determination was found to contain 22(2)% La, 24(2)% Ga, and 54(4)% Bi. Crystals removed from the reaction vessel and analyzed within 30 min on the scanning electron microscope after exposure to the atmosphere showed no oxygen contamination. The crystals are slightly air-sensitive and surface oxidation occurs within several hours. Attempts to substitute other RE elements for La in $LaGaBi_2$ have so far been unsuccessful. However, analysis of X-ray powder patterns reveals the presence of other unidentified phases different from $LaGaBi_2$. Efforts to identify these phases are ongoing.

Structure Determination. Weissenberg photography confirmed that the selected crystal was single and gave preliminary cell parameters. Intensity data were collected on a Bruker Platform/SMART 1000 CCD diffractometer at 22 °C using ω scans (0.2°) in the range $3.48° \le 2\theta$ (Mo Kα) $\le 65.18°$. Final cell parameters were refined from least-squares analysis of 3708 reflections. Crystal data and further details of the data collection are given in Table 1. All calculations were carried out with use of the SHELXTL (version 5.1) package.[23] Conventional atomic scattering factors and anomalous dispersion corrections were used.[24] Intensity data were processed, and face-indexed numerical absorption corrections were applied in XPREP.

Table 2. Positional and Equivalent Isotropic Displacement Parameters for $LaGaBi_2$

atom	Wyckoff position	x	y	z	U_{eq}^a (Å^2)
La	6*m*	0.225 30(3)	0.450 59(6)	1/2	0.0091(2)
Ga	6*k*	0.181 99(13)	0	1/2	0.0219(4)
Bi(1)	6*j*	0.324 57(5)	0	0	0.0128(2)
Bi(2)	3*g*	1/2	0	1/2	0.0143(2)
Bi(3)	2*c*	1/3	2/3	0	0.0097(2)
Bi(4)	1*a*	0	0	0	0.0176(3)

^{a} U_{eq} is defined as one-third of the trace of the orthogonalized $\mathbf{U}_{ij}$ tensor.

Table 3. Selected Interatomic Distances (Å) for $LaGaBi_2$

La−Ga	3.3840(13) (×2)	Ga−Ga	2.466(2) (×2)
La−Bi(1)	3.4419(3) (×4)	Ga−Bi(1)	2.9253(13) (×2)
La−Bi(2)	3.4363(2) (×2)	Bi(1)−Bi(2)	3.2366(5) (×2)
La−Bi(3)	3.3547(6) (×2)	Bi(4)−Ga	3.3024(13) (×12)

The centrosymmetric space group *P*6/*mmm* was chosen on the basis of the observed Laue symmetry 6/*mmm* and no systematic extinctions in the intensity pattern. Initial positions for all atoms were found by direct methods. A distinct feature of this structure is the presence of a twelve-coordinate site at the origin occupied by Bi atoms sandwiched between pairs of Ga_6 rings. Because the corresponding site in the closely related structure of $La_{13}Ga_8Sb_{21}$ is filled with La atoms,[21] the possibility of Bi and La disorder had to be carefully considered. When this site was allowed to be occupied by a mixture of Bi and La atoms, with the constraint that the sum of the occupancies equal unity, the values of the occupancies converged to 1.00(3) Bi and 0.00 La, with a reasonable U_{eq} value of 0.0177(4) Å^2. When the alternative model containing La atoms entirely at this site was refined, the U_{eq} value became very small (0.0005(7) Å^2) and $R(F)$ increased to 0.064. Finally, when all sites except Ga were allowed to be occupied by a mixture of Bi and La atoms, their occupancies (Bi/La) converged to 0.97(3)/0.02, 0.99(3)/0.00, 0.98(4)/ 0.02, and 1.02(3)/0.00 for the sites identified as Bi and 0.00(3)/1.07 for the site identified as La. These results constitute convincing evidence that the structure is ordered and that Bi, not La, occupies the twelve-coordinate site at the origin. The final formula $LaGaBi_2$ is also consistent with the EDX analysis. The displacement ellipsoids of the Ga atoms in the Ga_6 rings are somewhat elongated along the *c*-direction, but not to a sufficient degree to justify splitting into two sites, as occurs in the related structure of $La_{13}Ga_8Sb_{21}$.[21]

The final refinement gave $R(F) = 0.037$ and $R_w(F_o^2) = 0.076$ with reasonable anisotropic displacement parameters for all atoms. The final difference electron map is featureless ($\Delta\rho_{max} = 4.97$, $\Delta\rho_{min} = -3.59$ e$^-$ Å^{-3}). The atomic positions of $LaGaBi_2$ were standardized with the program STRUCTURE TIDY.[25] Final values of the positional and displacement parameters are given in Table 2. Interatomic distances are listed in Table 3. Further data in the form of a CIF file are available as Supporting Information, and final structural amplitudes are available from the authors.

Band Structure. A tight-binding extended Hückel band structure calculation was performed on fragments of the $LaGaBi_2$ structure with use of the EHMACC suite of programs.[26,27] The atomic

(20) Hulliger, F.; Ott, H. R. *J. Less-Common Met.* **1977**, *55*, 103.
(21) Mills, A. M.; Mar, A. *Inorg. Chem.* **2000**, *39*, 4599.
(22) Sologub, O.; Vybornov, M.; Rogl, P.; Hiebl, K.; Cordier, G.; Woll, P. *J. Solid State Chem.* **1996**, *122*, 266.
(23) Sheldrick, G. M. *SHELXTL*, version 5.1; Bruker Analytical X-ray Systems, Inc.: Madison, WI, 1997.
(24) *International Tables for X-ray Crystallography*; Wilson, A. J. C., Ed.; Kluwer: Dordrecht, The Netherlands, 1992; Vol. C.
(25) Gelato, L. M.; Parthé, E. *J. Appl. Crystallogr.* **1987**, *20*, 139.
(26) Whangbo, M.-H.; Hoffmann, R. *J. Am. Chem. Soc.* **1978**, *100*, 6093.
(27) Hoffmann, R. *Solids and Surfaces: A Chemist's View of Bonding in Extended Structures*; VCH: New York, 1988.

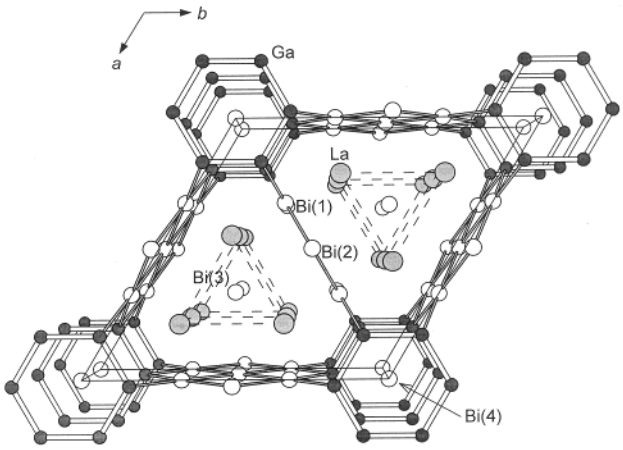

Figure 1. View of $LaGaBi_2$ down the *c*-axis showing the unit cell outline and the labeling scheme. The large lightly shaded circles are La atoms, the small solid circles are Ga atoms, and the medium open circles are Bi atoms. The dashed lines outline the assemblies of La_6 trigonal prisms.

parameters (valence shell ionization potentials H_{ii} (eV) and orbital exponents ζ_i), taken from literature values for intermetallic compounds with similar bonding character ($La_{13}Ga_8Sb_{21}$, $RE_{12}Ga_4Sb_{23}$, and Ti_4MBi_2),[28,29] were as follows: for Ga 4s, $H_{ii} = -14.58$, $\zeta_i = 1.770$; for Ga 4p, $H_{ii} = -6.75$, $\zeta_i = 1.550$; for Bi 6s, $H_{ii} = -15.19$, $\zeta_i = 2.560$; for Bi 6p, $H_{ii} = -7.70$, $\zeta_i = 2.072$. For the $[GaBi_2]^{3-}$ framework of $LaGaBi_2$, properties were extracted from the band structure using 50 *k* points in the irreducible portion of the Brillouin zone.

Electrical Resistivity. Single crystals of 0.025−0.040 cm length and 0.001−0.002 cm width were mounted in a four-probe configuration for ac resistivity measurements along the crystallographic *c* (needle) axis between 2 and 300 K on a Quantum Design PPMS system equipped with an ac-transport controller (Model 7100). A current of 0.1 mA and a frequency of 16 Hz were used.

X-ray Photoelectron Spectroscopy. A sample consisting of $LaGaBi_2$ crystals was pressed into indium foil and analyzed on a Kratos Ultra Axis X-ray photoelectron spectrometer using a monochromatized Al Kα source and a 10 eV pass energy. High-resolution spectra were taken for the Bi 4f, Ga $2p_{3/2}$, and Ga 3d peaks. Corrected binding energies were referenced to the C 1s peak at 285.0 eV arising from adventitious hydrocarbon. Additional peaks were observed at binding energies (158.8 eV for Bi $4f_{7/2}$, 1118.5 eV for Ga $2p_{3/2}$, and 18.9 eV for Ga 3d) characteristic of bismuth(III) and gallium(III) oxides, suggesting that surface oxidation occurred in the course of the analysis.

Results and Discussion

Structure. Figure 1 shows the structure of $LaGaBi_2$ viewed down the *c*-axis. A metalloid framework consisting of Ga and Bi atoms forms channels outlined by 15-membered rings. Three-atom-wide Bi ribbons are connected by Ga_6 rings to build up this framework. Within these channels are trigonal prisms whose vertexes are La atoms and which are centered by Bi atoms. These trigonal prisms share their triangular faces to form columns extending along the *c*-direction. The Ga_6 rings sandwich additional Bi atoms between them.

These Ga_6 rings are rigorously planar and have ideal bond angles of 120°. The Ga−Ga distances of 2.466(2) Å are significantly shorter than typical single-bond lengths found in other extended structures such as $Na_2Ga_3Sb_3$ (2.541(3) Å)[30] or $SmGaSb_2$ (2.539(2) Å).[31] Multiple-bonding character is invoked for Ga−Ga distances as short as 2.3−2.4 Å found in organometallic complexes, although these claims are often controversial.[32,33] Perhaps more relevant comparisons can be made to the intermetallic compounds $LaGa_2$ (AlB_2-type) in which planar hexagonal Ga nets are found (2.494 Å)[34] and CaGa (CrB-type) in which zigzag Ga chains are found (2.66 Å),[35] or to the cluster-containing compounds Na_7Ga_{13} (2.54(1) Å)[36] and $Na_{22}Ga_{39}$ (2.435(7) Å)[37] in which the shortened distance in the latter is attributed to formation of a Ga═Ga double bond.[38] More cogently, comparison to the closely related structure of $La_{13}Ga_8Sb_{21}$, where slightly puckered Ga_6 rings are also found (2.422(5) Å),[28] suggests that delocalized π-bonding is an equally important contribution to the Ga−Ga bonds in $LaGaBi_2$.

One-dimensional three-atom-wide Bi ribbons extend along the *c*-direction. The central Bi(2) atoms are bonded in a square-planar fashion to four surrounding Bi(1) atoms, as are the terminal Bi(1) atoms, which are bonded to two Bi(2) and two Ga atoms. The Bi(1)−Bi(2) distances are 3.2366(5) Å. Bi−Bi bond lengths are highly variable and are not easily correlated with bond strength; in some instances, matrix effects may be important. The distances in $LaGaBi_2$ are clearly comparable to those in Bi square nets found in $CeCu_{1-x}Bi_2$ (3.221(2) Å)[14] or $SrZnBi_2$ (3.28(1) Å),[8] or in the six-atom-wide Bi ribbon found in $HfBi_2$ (3.210(3)−3.289(3) Å within three-atom-wide ribbons connected by shorter 3.072(3) Å bonds),[18] where hypervalent multicenter bonding is undoubtedly occurring in a manner analogous to numerous antimonides. Similarly, the Bi_3^{7-} trimers in Zintl compounds such as $Eu_{14}MnBi_{11}$ contain relatively long Bi−Bi distances (3.397(1) Å) corresponding to $3c-4e^-$ bonds.[15] In compounds such as $Ca_{11}Bi_{10}$, which *ought* to be accountable by $2c-2e^-$ bonds, the Bi−Bi distances are not significantly shorter (3.15(3)−3.20(3) Å),[2] but packing effects have been invoked.[4] An even more puzzling case is Sr_2Bi_3 (3.13(1)−3.39(1) Å), which is apparently not an electron-precise compound.[3] Even in elemental Bi (3.072 Å intralayer vs 3.529 Å interlayer distances),[39] the existence of weaker intermediate bonding is indisputable.

There remain two types of isolated Bi atoms. The Bi(3) atoms are bonded to six La atoms in a trigonal prismatic fashion. In turn, the La atoms are coordinated to eight Bi and two Ga atoms and reside at centers of bicapped trigonal

(28) Mills, A. M.; Deakin, L.; Mar, A. *Chem. Mater.* **2001**, *13*, 1778.
(29) Rytz, R.; Hoffmann, R. *Inorg. Chem.* **1999**, *38*, 1609.
(30) Cordier, G.; Ochmann, H.; Schäfer, H. *Mater. Res. Bull.* **1986**, *21*, 331.
(31) Mills, A. M.; Mar, A. *J. Am. Chem. Soc.* **2001**, *123*, 1151.
(32) Power, P. P. *J. Chem. Soc., Dalton Trans.* **1998**, 2939.
(33) Power, P. P. *Chem. Rev.* **1999**, *99*, 3463.
(34) Kimmel, G.; Dayan, D.; Zevin, L.; Pelleg, J. *Metall. Trans. A* **1985**, *16*, 167.
(35) Merlo, F.; Fornasini, M. L. *J. Less-Common Met.* **1986**, *119*, 45.
(36) Frank-Cordier, U.; Cordier, G.; Schäfer, H. *Z. Naturforsch. B: Anorg. Chem. Org. Chem.* **1982**, *37*, 119.
(37) Ling, R. G.; Belin, C. *Acta Crystallogr. Sect. B: Struct. Crystallogr. Cryst. Chem.* **1982**, *38*, 1101.
(38) Burdett, J. K.; Canadell, E. *J. Am. Chem. Soc.* **1990**, *112*, 7207.
(39) Donohue, J. *The Structures of the Elements*; Wiley: New York, 1979.

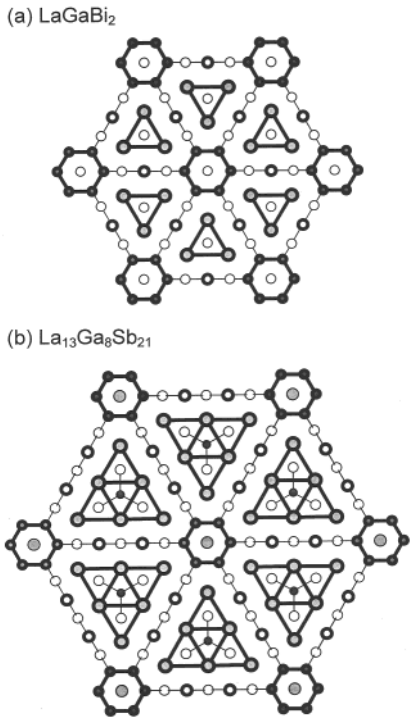

Figure 2. Comparison of the structures of (a) $LaGaBi_2$ and (b) $La_{13}Ga_8Sb_{21}$ shown in projection down the hexagonal *c*-axis. The large lightly shaded circles are La atoms, the small solid circles are Ga atoms, and the medium open circles are pnicogen atoms. Circles with thicker rims are atoms residing in planes displaced by *c*/2.

prisms similar to what occurs in $La_{13}Ga_8Sb_{21}$ and $Pr_{12}Ga_4Sb_{23}$.[21] The La−Bi (3.3547(6)−3.4419(3) Å) and La−Ga distances (3.3840(13) Å) are similar to those found in LaBi (3.289 Å)[40] and $LaGa_2$ (3.335 Å),[34] respectively. The Bi(4) atoms are unique, being sandwiched between pairs of Ga_6 rings and forming twelve Bi−Ga bonds at 3.3024(13) Å. To our knowledge, no Bi−Ga bond lengths have been reported in solid-state extended compounds. (The organometallic complexes $Et_3Ga-Bi(SiMe_3)_3$ and $(t\text{-}Bu)_3Ga-Bi(i\text{-}Pr)_3$ contain Bi−Ga bonds of 2.966(1) and 3.135(1) Å, respectively.[41] A $[GaBi_3]^{2-}$ cluster anion is known, but no coordinates were reported.[42]) An estimate can be obtained by calculating the bond-valence parameter for a Bi−Ga bond, 2.7 Å.[43] The longer observed distances in $LaGaBi_2$ are consistent with the very high CN of 12 around Bi(4).

Many intermetallic structures are built up of assemblies of filled trigonal prisms and can often be classified as different members of homologous series containing increasingly larger assemblies of these trigonal prisms. Figure 2 shows that the structures of $LaGaBi_2$ and $La_{13}Ga_8Sb_{21}$ are closely related in this manner, both having columns of La_6 trigonal prisms surrounded by a network of Ga_6 rings connected by *Pn* (pnicogen) ribbons. If *n* is used as an index so that n^2 equals the number of trigonal prisms within these assemblies, then $LaGaBi_2$ and $La_{13}Ga_8Sb_{21}$ correspond to the

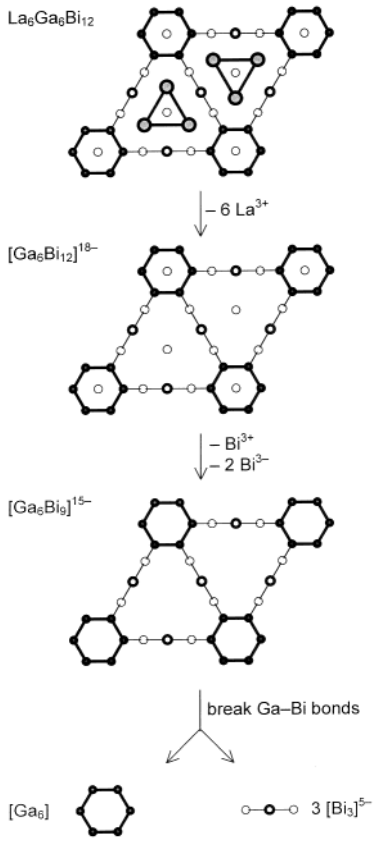

Figure 3. Retrotheoretical analysis of $LaGaBi_2$.

$n = 1$ and 2 members, respectively. The La_6 trigonal prisms are filled so that isolated Bi atoms occur in $LaGaBi_2$, whereas $GaSb_3$ trigonal planar units appear in $La_{13}Ga_8Sb_{21}$. An important difference is that the Ga_6 rings sandwich Bi atoms in $LaGaBi_2$ in contrast to La atoms in $La_{13}Ga_8Sb_{21}$.

Bonding. The three-dimensional structure of $LaGaBi_2$ is complex. To facilitate understanding of the bonding, the structure is broken down into smaller substructures through a retrotheoretical approach.[44] In this process, noninteracting atoms are sequentially removed or bonds are broken to give lower-dimensional substructures that are analyzed separately (Figure 3). Within the unit cell, the formula is $La_6Ga_6Bi_{12}$. Following the Zintl concept, the La atoms are assumed to transfer their valence electrons completely to the remaining metalloid framework. Removal of six La^{3+} ions leaves a charge of 18− on the covalent $[Ga_6Bi_{12}]$ framework. Of the four types of Bi atoms, Bi(3) and Bi(4) are isolated. Bi(3) is surrounded by electropositive La atoms, so it accepts electrons to attain an octet and achieves an oxidation state of 3−. In contrast, Bi(4) is surrounded by Ga atoms, which have similar electronegativity to Bi. It is appealing to assign an oxidation state of 3+ to Bi(4) as a starting point, especially when one considers that the analogous site in $La_{13}Ga_8Sb_{21}$ is occupied by La^{3+} and that trivalent Bi often substitutes for rare earths in many chalcogenides. Removal of one $Bi(4)^{3+}$ and two $Bi(3)^{3-}$ ions per unit cell leaves a charge of 15− in the remaining substructure $[Ga_6Bi_9]$. Finally, the $[Ga_6Bi_9]$ substructure could be further decomposed by breaking

(40) Nomura, K.; Hayakawa, H.; Ono, S. *J. Less-Common Met.* **1977**, *52*, 259.
(41) Kuczkowski, A.; Thomas, F.; Schulz, S.; Nieger, M. *Organometallics* **2000**, *19*, 5758.
(42) Xu, L.; Sevov, S. C. *Inorg. Chem.* **2000**, *39*, 5383.
(43) O'Keeffe, M.; Brese, N. E. *J. Am. Chem. Soc.* **1991**, *113*, 3226.
(44) Papoian, G.; Hoffmann, R. *J. Solid State Chem.* **1998**, *139*, 8.

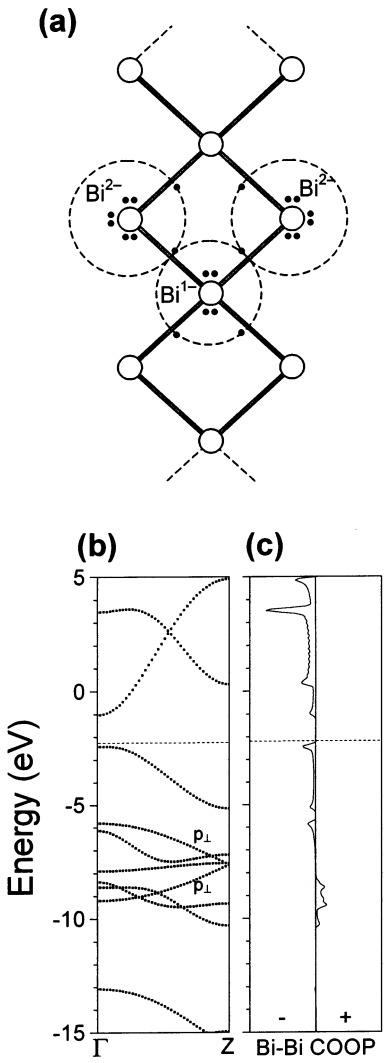

Figure 4. (a) Simple electron-counting scheme, with electron in each Bi−Bi bond being partitioned evenly, (b) band dispersion, and (c) Bi−Bi crystal orbital overlap population (COOP) curve for the one-dimensional $[Bi_3]^{5-}$ ribbon in $LaGaBi_2$. The dashed horizontal line marks the Fermi level.

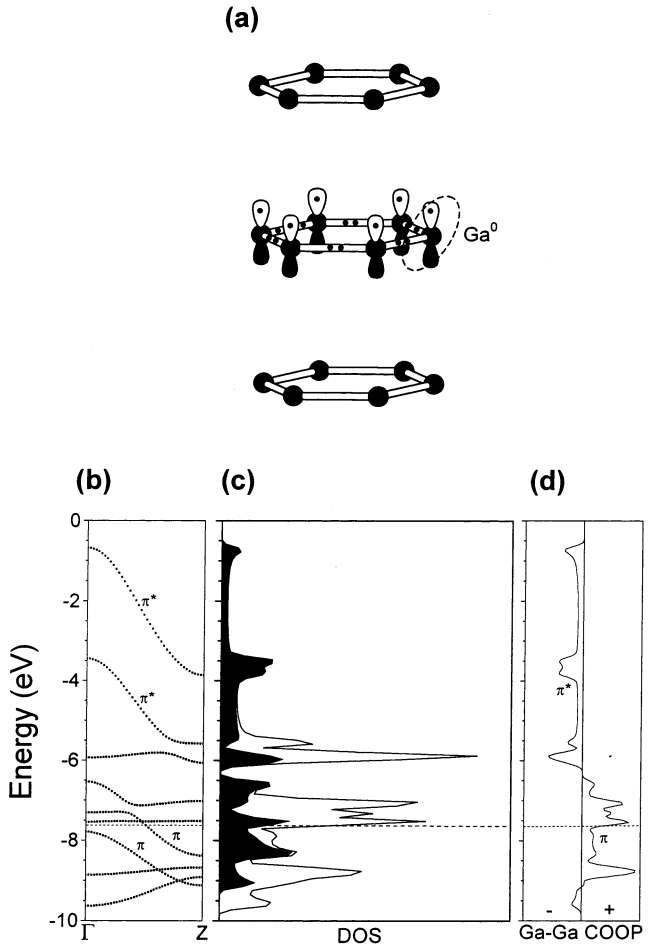

Figure 5. (a) Simple electron-counting scheme, (b) band dispersion, (c) density of states (DOS) (with the Ga p_z projection shown by the filled area), and (d) Ga−Ga COOP curve for the one-dimensional stack of Ga_6 rings in $LaGaBi_2$. The dashed horizontal line marks the Fermi level ($\epsilon_f = -7.6$ eV).

Ga−Ga bonds (in a similar fashion described in the case of $La_{13}Ga_8Sb_{21}$)[28] to give Ga_2Bi_3 ribbons, but the alternative viewpoint of breaking Ga−Bi bonds gives the more recognizable units of Ga_6 rings and $[Bi_3]$ ribbons.

The one-dimensional $[Bi_3]$ ribbon extending along the *c*-direction is reminiscent of similar ribbons seen in many antimonides. As with the corresponding Sb ribbons, the $[Bi_3]$ ribbon can be regarded as being either excised from an infinite two-dimensional square Bi net or fused from finite linear triatomic rods containing 3c−4e$^-$ bonds.[45,46] A stable electron count for a Bi_3 ribbon should be 20 e$^-$. The distribution of electrons conforms to the octet rule if each Bi−Bi bond is considered to be a one-electron bond, on average. As shown in Figure 4a, partitioning the shared electrons in these bonds evenly between pairs of Bi atoms gives rise to an oxidation state of 1− for the central Bi atom and 2− for the terminal Bi atoms, resulting in an overall charge of 5− for the $[Bi_3]$ ribbon. The band structure for the $[Bi_3]^{5-}$ ribbon, shown in Figure 4b, is similar to that for an $[Sb_3]^{5-}$ ribbon except that the energies of the bands are significantly higher (by about 5 eV).[44] Bonding and antibonding interactions develop through σ-overlap of the in-plane p-orbitals of the Bi atoms, accounting for the dispersion of bands from −10 to +5 eV. The out-of-plane p-orbitals remain relatively localized in energy between −9 and −6 eV, accommodating one of the lone pairs on each Bi atom. At a count of 20 e$^-$, some Bi−Bi antibonding levels are occupied, as seen in the COOP curve (Figure 4c), giving a small but positive overlap population of 0.12. The Mulliken charges are 0.74− for the central Bi atom and 2.13− for the terminal Bi atoms, consistent with the simple electron-counting scheme shown in Figure 4a.

The Ga_6 rings are arranged in a one-dimensional stack along the *c*-direction (Figure 5a), but the inter-ring distance is very long (equal to the *c*-parameter, 4.3937(1) Å). As a starting point, surrounding each Ga atom with two bond pairs and two lone pairs to achieve an octet gives an oxidation state of 3−. Each Ga atom is actually also bonded to two Bi atoms above and below the plane of the ring, but, in the deconstruction process (Figure 3), these bonds were broken heterolytically. Two electrons from a lone pair on each Ga

(45) Papoian, G. A.; Hoffmann, R. *Angew. Chem., Int. Ed.* **2000**, *39*, 2408.
(46) Papoian, G.; Hoffmann, R. *J. Am. Chem. Soc.* **2001**, *123*, 6600.

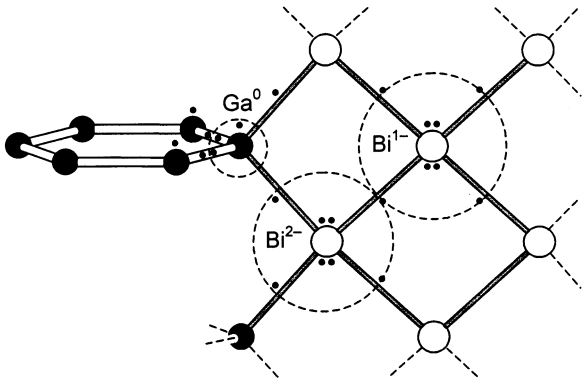

Figure 6. Electron-counting scheme for connection of $[Bi_3]^{5-}$ ribbon with $[Ga_6]$ stack, with oxidation-state assignments shown.

atom are formally transferred to the $[Bi_3]$ ribbon in this analysis, giving an oxidation state of 1−. The remaining lone pair can be assumed to occupy a p_z orbital on each Ga atom. If π-bonding is to be an important contribution, one electron of this pair must be removed to ensure that no Ga−Ga π-antibonding levels are occupied, resulting in an oxidation state of 0 for each Ga atom (Figure 5a). The band structure and DOS curve for a stack of Ga_6 rings are shown in Figure 5b,c. The projection of Ga p_z orbitals, perpendicular to the plane of the ring, is indicated by the filled portion of the DOS curve. As expected, this can be traced to Ga−Ga π-bonding levels from −9.5 to −6.5 eV and π-antibonding levels from −6.5 to −0.5 eV, as confirmed by the COOP curve (Figure 5d). The overlap population of 0.79 for the intra-ring Ga−Ga distance of 2.466(2) Å is substantial, in contrast to a value of 0.04 for the inter-ring distance of 4.394 Å.

The $[Bi_3]^{5-}$ ribbon can now be recombined with the stacks of Ga_6 rings to form the $[Ga_6Bi_9]^{15-}$ substructure. The Fermi levels for the separated $[Bi_3]^{5-}$ ribbons and $[Ga_6]$ stacks are very different, an artifact of the decision to assign the bonding electrons in the Ga−Bi bonds entirely to the more electronegative Bi atoms in Figure 3. Because the electronegativities of Ga and Bi differ by only 0.2 Pauling units, these bonds are actually strongly covalent. Each Ga atom has an acceptor orbital (approximately an sp^2 hybrid) oriented external to the ring. Electron density is then transferred from the terminal Bi atoms of the $[Bi_3]$ ribbon back to the Ga_6 rings, equalizing the Fermi level and forming 3c−2e$^-$ bonds in the process, as schematized in Figure 6. We can proceed directly to the results of the calculation on the $[Ga_6Bi_{12}]^{18-}$ substructure as inclusion of the remaining isolated Bi atoms in the rest of the structure changes little of the conclusions. Figure 7 shows the DOS and COOP curves for the full covalent framework $[Ga_6Bi_{12}]^{18-}$. As anticipated, there is considerable mixing of Ga and Bi states, giving rise to a very broad DOS curve with significant contributions from both elements in the entire energy range. The Ga−Ga bond remains strong (overlap population 0.755) through occupation of bonding levels that include a π-bonding component involving overlap of p_z orbitals (Figure 7b). For comparison, the 2c−2e$^-$ Ga−Ga bonds (2.539(2) Å) in the zigzag Ga chains of $SmGaSb_2$ have an overlap population of 0.58.[31] A bond order of approximately 1.5 for the Ga−Ga bonds in the Ga_6 ring is therefore not unrealistic. The 2.925(1) Å bond between Ga and Bi(1) (the terminal atoms on the $[Bi_3]$ ribbons) is essentially optimized (Figure 7c) and strong (overlap population 0.55). The longer 3.302(1) Å bond between Ga and Bi(4) (the atoms sandwiched between Ga_6 rings) is much weaker (overlap population, 0.06). The Bi−Bi bond is strengthened somewhat (overlap population, 0.25) when the $[Bi_3]$ ribbons are involved in the entire covalent framework than when they are isolated, as a result of the back-transfer of electron density mentioned above, thereby depopulating some antibonding Bi−Bi levels (cf. Figures 7d and 4c).

In the deconstruction process, we assigned oxidation states to give the formulation $(La^{3+})_6(Ga^0)_6(Bi(1)^{2-})_6(Bi(2)^{-})_3(Bi(3)^{3-})_2(Bi(4)^{3+})$. There is evidence that even La can participate in some degree of covalent bonding with other atoms,[28] and indeed, a Hückel calculation involving the full structure including the La atoms suggests that the La−Bi bonds have significant covalent character (overlap population, 0.400). Nevertheless, the assumption of La^{3+} is useful to keep. The Mulliken charges for the other atoms are found to be −0.77 for Ga, −0.75 for Bi(1), −0.90 for Bi(2), −3.00 for Bi(3), and −0.16 for Bi(4). Consistent with the high

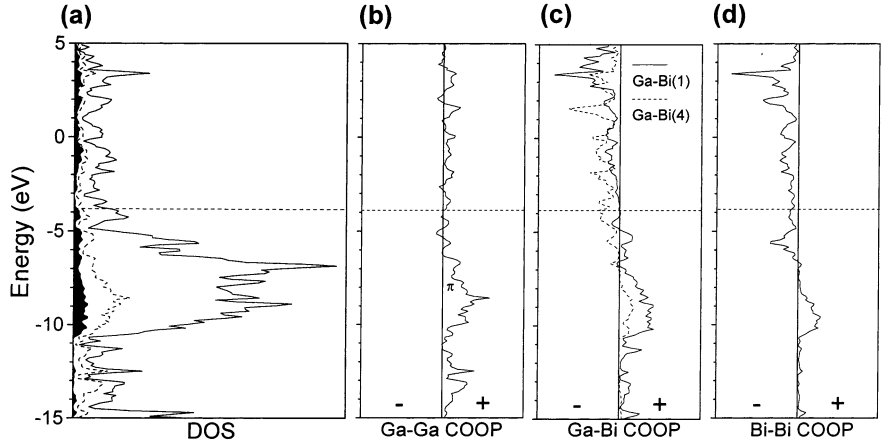

Figure 7. (a) Density of states (DOS) (with the Ga projection shown by the dashed line and the Ga p_z projection shown by the filled area of the curve; what remains of the DOS is the Bi projection) and (b) Ga−Ga, (c) Ga−Bi, and (d) Bi−Bi COOP curves for the three-dimensional $[Ga_6Bi_{12}]^{18-}$ substructure in $LaGaBi_2$. The dashed horizontal line marks the Fermi level ($\epsilon_f = -3.8$ eV).

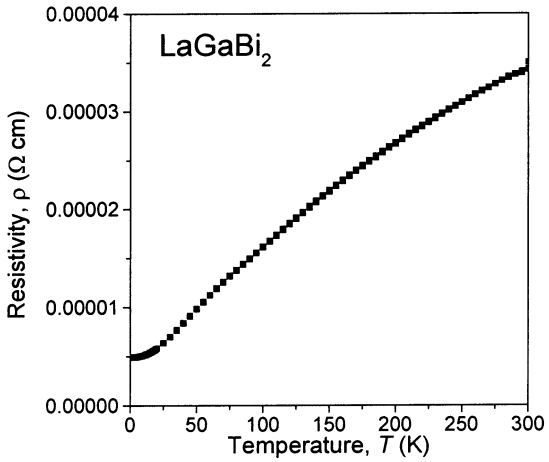

Figure 8. Temperature dependence of the resistivity along the needle axis *c* of a single crystal of $LaGaBi_2$.

degree of covalent character of bonding really present in the structure, the charges are much less extreme than would be suggested by an oxidation-state formalism. The X-ray photoelectron spectra indicate binding energies of 1116.6 eV (Ga $2p_{3/2}$), 18.3 and 18.9 eV (Ga 3d doublet), and 156.6 and 161.9 eV (Bi $4f_{7/2}$ and $4f_{5/2}$) in $LaGaBi_2$ that are close to the low end of ranges of binding energies reported for elemental Ga and Bi.[47] This observation, along with the inability to resolve by XPS the formally different types of Bi atoms in the structure, supports the assertion that the Ga and Bi atoms in the structure are really in reduced states rather than acting as cations and that the Ga−Bi bonds are really strongly covalent.

As predicted by the band structure calculation, $LaGaBi_2$ is metallic with the resistivity decreasing only slightly with decreasing temperature (Figure 8). In contrast to the closely related structure of $La_{13}Ga_8Sb_{21}$, it is not superconducting.

$LaGaBi_2$ is noteworthy in that both strong bonding in Ga−Ga bonds (involving a π-overlap contribution so that the bond order is about 1.5) and weak multicenter bonding in Ga−Bi ($3c-2e^-$) and Bi−Bi ($2c-1e^-$) bonds are implicated. The occurrence of one-dimensional Bi ribbons, previously only seen in $ZrBi_2$ and $HfBi_2$,[17,18] suggests that this structural theme may be more general and can be extended from antimonides to bismuthides, allowing us to predict new target structures.

Acknowledgment. The Natural Sciences and Engineering Research Council of Canada and the University of Alberta supported this work. We thank Dr. Robert McDonald (Faculty Service Officer, X-ray Crystallography Laboratory) for the X-ray data collection, Ms. Christina Barker (Department of Chemical and Materials Engineering) and Mr. George Braybrook (Department of Earth and Atmospheric Sciences) for assistance with the EDX analyses, and Mr. Mark Biesinger (Surface Science Western, University of Western Ontario) for the XPS analysis.

Supporting Information Available: An X-ray crystallographic file in CIF format for the structure of $LaGaBi_2$. This material is available free of charge via the Internet at http://pubs.acs.org.

IC020413W

(47) Wagner, C. D.; Naumkin, A. V.; Kraut-Vass, A.; Allison, J. W.; Powell, C. J.; Rumble, J. R., Jr. *NIST X-ray Photoelectron Spectroscopy Database*, version 3.2 (web version); National Institute of Standards and Technology: Gaithersburg, MD, 2000 (http://srdata.nist.gov/xps).